Large-Scale Pharmacokinetic Reconstruction of Propofol Effect-Site Concentrations:

Quantifying the Divergence between Clinical Titration and Age-Dependent Pharmacodynamic Requirements

Brent Ershoff, MD
Department of Anesthesiology and Perioperative Medicine,
University of California, Los Angeles

Abstract

Background: Propofol dosing guidelines recommend age-based reductions because hypnotic sensitivity increases in older adults. Most real-world evaluations of induction practice, however, have relied on total weight-normalized dose (mg/kg) rather than estimating cerebral exposure using pharmacokinetic models. Because age-related pharmacokinetic changes alter the relationship between administered dose and peak effect-site concentration ($C_{e,max}$), mg/kg surrogates may misrepresent true age-dependent exposure during induction.

Methods: A retrospective reconstruction of 250,640 adult anesthetic inductions was performed using high-fidelity EHR medication timestamps. Propofol effect-site concentration trajectories were simulated at 1-second resolution using the Eleveld model. $C_{e,max}$ was benchmarked against age-adjusted hypnotic requirements (Ce_{50}) derived from the Eleveld model (standardized to a target Bispectral Index ≈ 47). Age–exposure relationships were estimated using covariate-adjusted natural cubic splines, controlling for BMI, sex, and ASA physical status.

Results: From young adulthood (18–24 years) to the oldest cohort (85–89 years), weight-normalized induction doses were reduced by 32% (3.16 to 2.16 mg/kg). However, modeled $C_{e,max}$ declined by only 17% (3.70 to 3.06 μg/mL), while the estimated physiological requirement declined by 34% (3.37 to 2.21 μg/mL), creating a widening titration offset with age. At age 75, the adjusted probability of exceeding the individual hypnotic requirement was 89.6% (95% CI: 89.3–89.8%). Notably, 54.7% (95% CI: 54.2–55.2%) of 75-year-old patients achieved peak exposures exceeding the average requirement of a healthy 20-year-old, indicating persistent anchoring of exposure to youthful levels. Findings were robust across model specifications and inclusion criteria.

Conclusions: In over a quarter-million inductions, real-world age-based dose reductions did not produce proportional reductions in peak propofol brain exposure. Achieved concentrations declined far more slowly than modeled geriatric sensitivity increases, consistent with systematic over-exposure in older adults. These findings suggest that weight-based dosing heuristics inadequately capture age-dependent exposure and support a transition toward exposure-informed and neurophysiologically guided induction titration in geriatric anesthesia.

INTRODUCTION

Older adults represent a rapidly expanding surgical population with millions undergoing procedures that require general anesthesia each year[1–3]. Aging is accompanied by clinically important pharmacodynamic changes in hypnotic sensitivity: for a given propofol exposure, older patients achieve loss of consciousness at significantly lower effect-site concentrations than younger cohorts, reflecting a profound age-dependent shift in neural sensitivity.[4]. Classic dose-finding studies established a monotonic decline in the propofol effect-site concentration required for loss of consciousness (C_{e50}) as a function of age—a relationship now codified in contemporary pharmacokinetic-pharmacodynamic (PK-PD) frameworks used for target-controlled infusion[5]. These pharmacodynamic observations underpin widely taught recommendations to reduce propofol dosing in older adults and are reflected in the product label that recommends lower induction doses in geriatric patients, in part to mitigate hypotension, excessive hypnotic depth, and downstream complications[6].

Despite strong physiologic rationale, induction practice in the real-world may not consistently translate age-related pharmacodynamic knowledge into bedside titration. Previous audits and registry studies suggest that many older adults receive induction doses that exceed the recommended ranges on the label[7–10]. However, a critical unresolved question remains: does bedside dosing—even when ostensibly reduced—produce an effect-site concentration trajectory that mirrors the known decline in physiologic requirement? While clinicians may down-titrate absolute doses for older adults, the magnitude of these reductions may fail to keep pace with the exponential increase in hypnotic sensitivity. In other words, a reduction in the mass of drug administered may not yield a commensurate reduction in brain exposure, potentially masking a systematic overshoot in geriatric patients.

A key limitation of many prior studies is the reliance on static exposure metrics, such as weight-based dose (mg/kg), as the primary measure of propofol effect[7]. Static metrics ignore the temporal resolution of drug delivery; a single rapid bolus and a fractionated induction may involve identical cumulative doses yet produce profoundly different peak effect-site concentrations. Furthermore, simple weight-based scaling fails to account for the dynamic covariate structures within validated pharmacokinetic models. In these frameworks, age- and body-composition-dependent changes in compartment volumes and clearances fundamentally alter the trajectory of the effect-site concentration. Consequently, dose-based audits likely provide an incomplete—and potentially misleading—estimate of anesthetic exposure, that may underestimate the degree of clinically significant overexposure in the elderly.

To evaluate whether clinical practice achieves age-appropriate propofol exposure, it is necessary to concentration rather than dose. While effect-site concentration is directly available in prospective target-controlled infusion (TCI) studies[11,12], such information is rarely available in large retrospective cohorts dominated by manual bolus dosing and heterogeneous administration techniques . In this study, high-resolution electronic medication timestamps were leveraged to reconstruct longitudinal, patient-specific propofol effect-site concentration trajectories at an unprecedented scale. The primary objective was to characterize the relationship between patient age and the maximum estimated effect-site concentration ($C_{e,\max}$)

achieved during induction, comparing these observed exposures to the age-adjusted C_{e50} requirements predicted by established pharmacodynamic frameworks.[13]. The analysis additionally evaluated whether conventional mg/kg dosing trends mirror modeled changes in effect-site exposure, testing the hypothesis that age-related reductions in administered induction doses are disproportionate to—and ultimately insufficient to offset—the pharmacokinetic and pharmacodynamic shifts that dictate actual cerebral exposure in the elderly.

METHODS

Study design and data source

This retrospective observational study was reviewed by the UCLA Institutional Review Board (IRB# 26-0331) and was determined to be exempt from oversight as it did not meet the regulatory definition of human subjects research. All analyses were conducted using a de-identified dataset. Data were obtained from the institutional perioperative data warehouse, a robust repository that aggregates high-fidelity anesthesia documentation, medication administration records, and physiological timestamps from the electronic medical record[14].

Study population and exclusions

We identified adult surgical cases (age $\geq$ 18 years) documented as receiving general anesthesia with propofol. Of the 258,741 initial cases, those with documented dose errors, missing simulation variables, or physiological outliers were sequentially excluded (Figure 1). Because the source system recorded all patients aged $\geq$ 90 years as age 90, the primary analysis was restricted to a cohort of 250,640 patients aged 18–89 years. Exclusion criteria were designed to ensure model integrity; however, the impact of these exclusions was evaluated in secondary sensitivity analyses described below.

Data Extraction and dosing metrics

Propofol administration records were retrieved from the perioperative data warehouse using Structured Query Language (SQL), with the cohort restricted to cases in which the documented "induction" event preceded the "intubation" timestamp. For each included case, the induction timestamp served as the primary reference point. To capture the full trajectory of the induction phase, all propofol administrations occurring within a 10-minute window following this event were extracted. This dataset included discrete bolus doses (mg) and continuous infusions, characterized by start/stop times and rate changes (μg/kg/min). Each event was recorded with its associated high-fidelity timestamp and dosing units to facilitate subsequent pharmacokinetic reconstruction.

To contextualize modeled effect-site exposure against conventional clinical practice, weight-normalized induction doses (mg/kg) were calculated using adjusted body weight (ABW). Ideal body weight (IBW) was determined using the Devine formula; for patients whose total body weight (TBW) exceeded 120% of their IBW, ABW was calculated as:

$$\text{ABW} = \text{IBW} + 0.4, (\text{TBW} - \text{IBW})$$

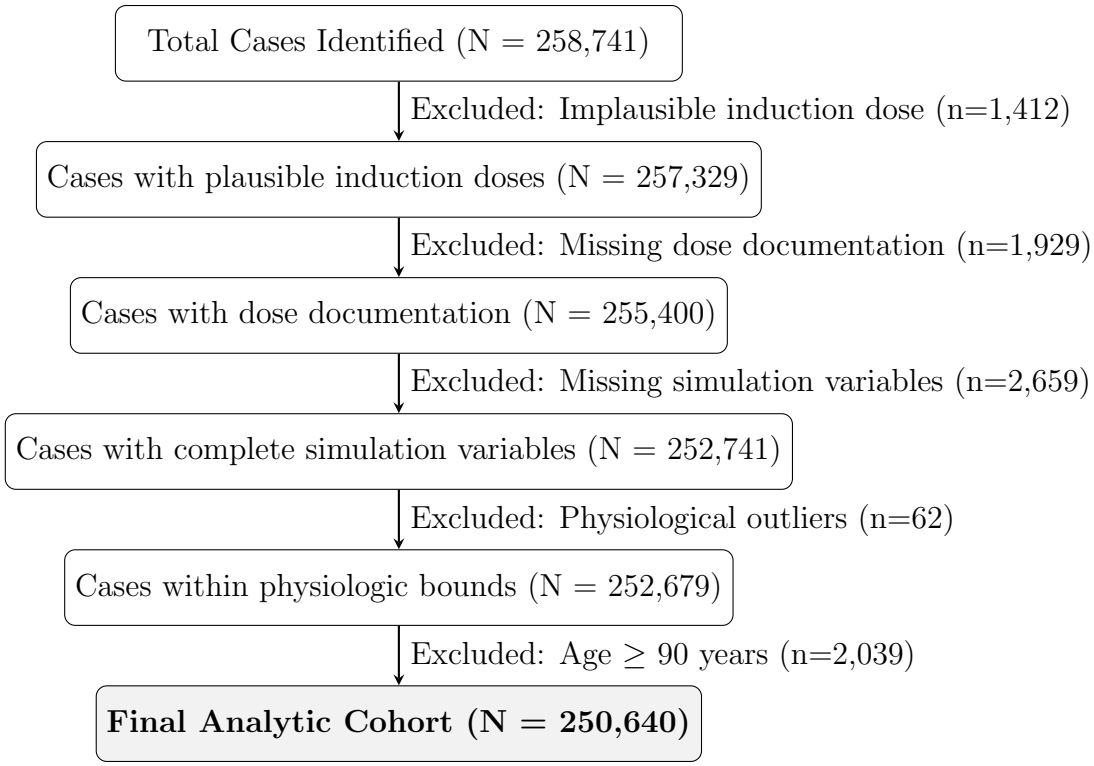

Figure 1: **CONSORT flow diagram.** Patient selection and exclusion process for the final analytic cohort.

For patients not meeting the 120% threshold, TBW was used as the dosing weight. The total induction dose (mg) within the extraction window was then normalized to ABW.

Pharmacokinetic Reconstruction

Effect-site concentration time series was reconstructed by simulating validated propofol PK/PD models forward in time using the observed medication event log as the input. Simulations were implemented using PyTCI, an open-source library for target-controlled infusion modeling.[15] The Eleveld model was selected as the primary estimator because its parameterization incorporates age and body-composition covariates across a broad ranges of age and BMI present in our cohort.[13] Patient-specific model parameters were determined from age, sex, height, and weight.

For each case, medication events were time-aligned to the first recorded propofol administration ($t = 0$), with subsequent event times represented as integer seconds relative to this first dose. Concentrations were subsequently simulated at 1-second resolution for a fixed 900-second (15-minute) horizon beginning at t=0. Between medication events, the model advanced in 1-second steps; during these intervals, any ongoing infusion contributed continuous drug input at the current rate while the PK state evolved. Bolus administrations recorded in mg were applied instantaneously. Infusion rates recorded in μg/kg/min were converted to mg/s and applied continuously until updated by a subsequent rate-change event. The primary exposure metric was the peak modeled effect-site concentration during

the 900-second window:

$$C_{e,\max} = \max_{t \in [0,900\ \mathrm{s}]} C_e(t).$$

To ensure the robustness of our findings against specific modeling assumptions and data-cleaning thresholds, several sensitivity analyses were performed. First, the full reconstruction workflow was repeated using the Schnider propofol model[16] to evaluate model-dependency. Additionally, the primary regression models were re-estimated without covariate adjustment for ASA physical status, BMI, or sex to verify that the observed age-related trajectories remained robust in unadjusted analysis. Next, the analysis was repeated including all documented propofol administrations—including those initially flagged as implausible—with missing dose values imputed as 0 mg. Finally, a secondary analysis was conducted to evaluate the consistency of the findings when incorporating the age 90 age cohort, which represents a single administrative aggregate of all patients aged 90 years and older whose specific chronological ages were masked for de-identification.

Statistical analysis and visualization

Statistical analyses were performed using Python (version 3.12.12)[17]. Data management and numerical computations were conducted using the pandas (version 2.2.2)[18] and NumPy (version 2.0.2)[19] libraries. Multivariable regression modeling and spline design matrices were implemented using the statsmodels (version 0.14.6)[20]and patsy (version 1.0.2)[21] libraries, respectively. The association between age and peak effect-site concentration ($C_{e,\max}$) was modeled using ordinary least squares (OLS) regression. To account for the known non-linear relationship between age and anesthetic requirements, age was modeled using a flexible B-spline with five degrees of freedom. To isolate the independent impact of aging on achieved concentrations, the covariate-adjusted relationship between age and effect-site exposure was estimated using marginal predictive effects. A standardized patient profile was defined, in which ASA physical status, BMI, and sex were held constant at their global cohort-level means. For visualization, these relationships were displayed as continuous adjusted spline curves and discrete binned estimates. These binned estimates represent the model-predicted concentrations (and 95% confidence intervals) for the standardized patient profile evaluated at the mean age of each pre-specified age stratum (18–24, 25–34, 35–44, 45–54, 55–64, 65–74, 75–84, and 85–89 years). This approach allows for the direct comparison of anesthetic exposure across the adult lifespan while controlling for the confounding influence of body habitus and comorbidity burden.

Pharmacodynamic reference and divergence analysis

To provide a standardized physiological anchor for evaluating age-dependent sensitivity, observed $C_{e,max}$ values were benchmarked against the age-adjusted Ce_{50} reference relationship derived from the Eleveld model:

$$Ce_{50}(\mathrm{Age}) = 3.08 \cdot e^{-0.00635,(\mathrm{Age}-35)}.$$

In the propofol-only configuration, this relationship characterizes the effect-site concentration associated with a Bispectral Index (BIS) of 47—a validated population-average requirement for surgical-depth anesthesia. This curve was utilized primarily as a reference slope to

quantify the relative divergence between clinician-titrated exposure and the model-predicted increase in hypnotic potency across the lifespan. Divergence between clinical practice and physiological requirements was characterized using three complementary approaches:

1. **Relative Divergence (Normalization):** To visualize the decoupling of dose titration from concentration requirements, $C_{e,\max}$, weight-normalized dose (mg/kg ABW), and the Ce_{50} target were indexed to the 18–24 year-old cohort (defined as 100%). This allowed for a direct comparison of the relative percentage decline in dosing effort versus the relative decline in biological requirement across the adult lifespan.

2. **Probability of Overexposure:** "Overexposure" was defined as any instance where an individual's $C_{e,\max} > Ce_{50}(\text{Age})$. The age-dependent probability of overexposure was modeled using logistic regression with B-spline terms for age, adjusted for sex, BMI, and ASA status. Standardized risk curves were generated by evaluating the model at the cohort-level means for all covariates.

3. **Young Adult Benchmark:** As a measure of titration anchoring, the probability that an older patient's $C_{e,max}$ exceeded the model-predicted Ce_{50} for a 21-year-old (3.37 $\mu g/mL$) was calculated. This benchmark was utilized to represent the likelihood of an elderly patient receiving a cerebral exposure equivalent to the theoretical surgical-depth requirement of a healthy young adult, thereby quantifying the extent to which clinical titration remains anchored to youthful dosing norms.

Logistic regression was utilized to model both binary outcomes (probability of overexposure and probability of exceeding the youthful benchmark) as a function of age using B-splines. Models were adjusted for sex, BMI, and ASA status, with standardized risk curves generated by evaluating results at cohort-level means for all covariates. For both analyses, modeled curves were overlaid with raw observed proportions within each age bin to provide clinical context alongside the covariate-adjusted results.

RESULTS

A total of 258,741 anesthetic cases were identified from the UCLA perioperative data warehouse. After applying eligibility criteria—including age $\geq$ 18 years and a minimum anesthetic duration of 30 minutes—and excluding cases with missing simulation variables or physiologically implausible anthropometrics, 250,640 unique cases comprised the final analytic cohort (Figure 1). Baseline demographic characteristics and clinical metrics for the study population are summarized in table 1.

Modeled effect-site concentrations (primary outcome)

To isolate the independent effect of aging, predicted peak effect-site concentrations ($C_{e,\max}$) and induction doses (mg/kg ABW) were generated for a standardized population profile. Across the adult lifespan, observed $C_{e,max}$ trajectories demonstrated a sustained elevation that diverged from the anticipated decline in age-related pharmacodynamic requirements. In covariate-adjusted analyses, $C_{e,\max}$ remained substantially above the Ce_{50} reference across all

Table 1: **Demographics and Induction Practice by Age Stratum.** Detailed breakdown of the study population across eight age cohorts. Values are presented as Mean (SD) or N (%).

Part A: Ages 18–55

	18-24 (N=15,004)	25-34 (N=27,208)	35-44 (N=33,610)	45-54 (N=39,770)
Age (Years)	21.0 (2.0)	29.8 (2.9)	39.6 (2.9)	49.7 (2.9)
Weight (kg)	72.4 (20.6)	77.5 (22.3)	80.4 (22.8)	81.2 (21.7)
Body Mass Index (kg/m^2)	25.0 (6.3)	26.8 (7.0)	27.8 (7.1)	28.1 (6.7)
Female Sex, N (%)	7,404 (49.3%)	14,816 (54.5%)	19,623 (58.4%)	22,292 (56.1%)
ASA Physical Status				
ASA 1	32.9%	23.2%	13.9%	6.1%
ASA 2	41.1%	46.1%	51.0%	48.6%
ASA 3	22.3%	26.1%	30.0%	38.6%
ASA 4	3.1%	4.0%	4.6%	6.0%
Infusion Administered, N (%)	1,836 (12.2%)	3,516 (12.9%)	4,776 (14.2%)	5,707 (14.4%)
>1 Bolus During Induction, N (%)	7,267 (48.4%)	12,659 (46.5%)	15,291 (45.5%)	17,650 (44.4%)

Part B: Ages 55–89

	55-64 (N=51,753)	65-74 (N=52,886)	75-84 (N=25,969)	85-89 (N=4,440)
Age (Years)	59.6 (2.9)	69.2 (2.8)	78.6 (2.7)	86.6 (1.4)
Weight (kg)	80.6 (20.7)	78.0 (19.0)	74.1 (16.9)	68.5 (15.1)
Body Mass Index (kg/m^2)	27.7 (6.3)	27.1 (5.8)	26.2 (5.1)	24.9 (4.7)
Female Sex, N (%)	25,416 (49.1%)	24,767 (46.8%)	12,022 (46.3%)	2,174 (49.0%)
ASA Physical Status				
ASA 1	2.1%	0.6%	0.1%	0.0%
ASA 2	39.9%	31.6%	21.1%	12.3%
ASA 3	49.1%	58.3%	68.7%	74.3%
ASA 4	8.2%	8.8%	9.3%	12.7%
Infusion Administered, N (%)	7,840 (15.1%)	8,323 (15.7%)	3,689 (14.2%)	592 (13.3%)
>1 Bolus During Induction, N (%)	22,299 (43.1%)	23,196 (43.9%)	11,737 (45.2%)	1,913 (43.1%)

age strata (Figure 2A). While the physiological requirement (Ce_{50}) decreased by 34%—dropping from 3.37 μg/mL in the 18–24 cohort to 2.21 μg/mL in the 85–89 cohort—the achieved peak brain concentration only declined by 17% (from 3.70 to 3.06 μg/mL).This resulting divergence occurred despite a significant 32% reduction in weight-normalized induction doses by clinicians (from 3.16 mg/kg in the youngest cohort to 2.16 mg/kg in the 85–89 group) Figure 2B). These findings suggest that while clinicians actively down-titrate mg/kg doses for older patients, the magnitude of these reductions is insufficient to offset the concurrent age-related shifts in pharmacokinetics and potency, leading to a progressive relative overexposure in the geriatric population.

Table 2: **Age-Stratified Propofol Induction Doses, Modeled Peak Concentrations, and Physiological Requirements.** Summary of covariate-adjusted induction doses (mg/kg) and resulting peak effect-site concentrations ($C_{e,\max}$, μg/mL) compared to age-adjusted Ce_{50} benchmarks across the adult lifespan. Values in parentheses represent 95% confidence intervals. Induction doses are standardized to mean ASA physical status, BMI, and sex. The "Surplus %" represents the percentage by which the modeled peak C_e exceeds the age-adjusted Ce_{50} for loss of consciousness.

Age Cohort	N	Induction Dose (mg/kg)	Peak C_e (95% CI)	Target Ce_{50}	Surplus (95% CI)
18-24	14,941	3.16 (3.14–3.17)	3.70 (3.69–3.72)	3.37	10.1% (9.6–10.5%)
25-34	27,088	3.08 (3.07–3.09)	3.78 (3.77–3.79)	3.18	18.6% (18.3–19.0%)
35-44	33,469	2.99 (2.98–3.00)	3.80 (3.79–3.81)	2.99	27.2% (26.9–27.4%)
45-54	39,583	2.89 (2.88–2.90)	3.79 (3.78–3.80)	2.80	35.1% (34.8–35.4%)
55-64	51,510	2.79 (2.78–2.79)	3.74 (3.74–3.75)	2.63	42.1% (41.8–42.4%)
65-74	52,594	2.66 (2.65–2.67)	3.64 (3.63–3.65)	2.48	46.9% (46.6–47.2%)
75-84	25,816	2.46 (2.45–2.47)	3.42 (3.41–3.43)	2.34	46.6% (46.1–47.1%)
85-89	4,419	2.16 (2.13–2.18)	3.06 (3.04–3.09)	2.22	38.1% (36.9–39.3%)

Despite these clinical reductions, the mean induction dose in patients aged 75–84 remained notably high at 2.46 mg/kg ABW. The divergence between titration efforts and physiological requirements is most clearly illustrated when normalizing all variables to the 18–24 year-old baseline (Figure 2C). While clinicians reduced weight-normalized doses by 32%—a reduction that nominally tracks the 34% decline in the Ce_{50} benchmark—the resulting peak effect-site concentration ($C_{e,max}$) decreased by only 17%.This illustrates a profound pharmacokinetic decoupling: even when clinicians attempt to mirror the anticipated decline in geriatric sensitivity through proportional mg/kg dose reductions, the resulting cerebral exposure remains at 83% of young-adult levels. Essentially, the typical 85-year-old in this cohort received nearly the same peak anesthetic intensity as a 20-year-old, despite the well-characterized age-related decline in the threshold for hypnotic effect. Comprehensive age-stratified summaries of induction doses, achieved peak effect-site concentrations ($C_{e,\max}$), and their respective 95% confidence intervals are provided in table 2. Notably, the extremely narrow confidence intervals across all age deciles reflect the high precision of the effect-size estimates afforded by the large cohort size, confirming that the observed exposure-requirement mismatch represents a systematic clinical pattern rather than stochastic variability.

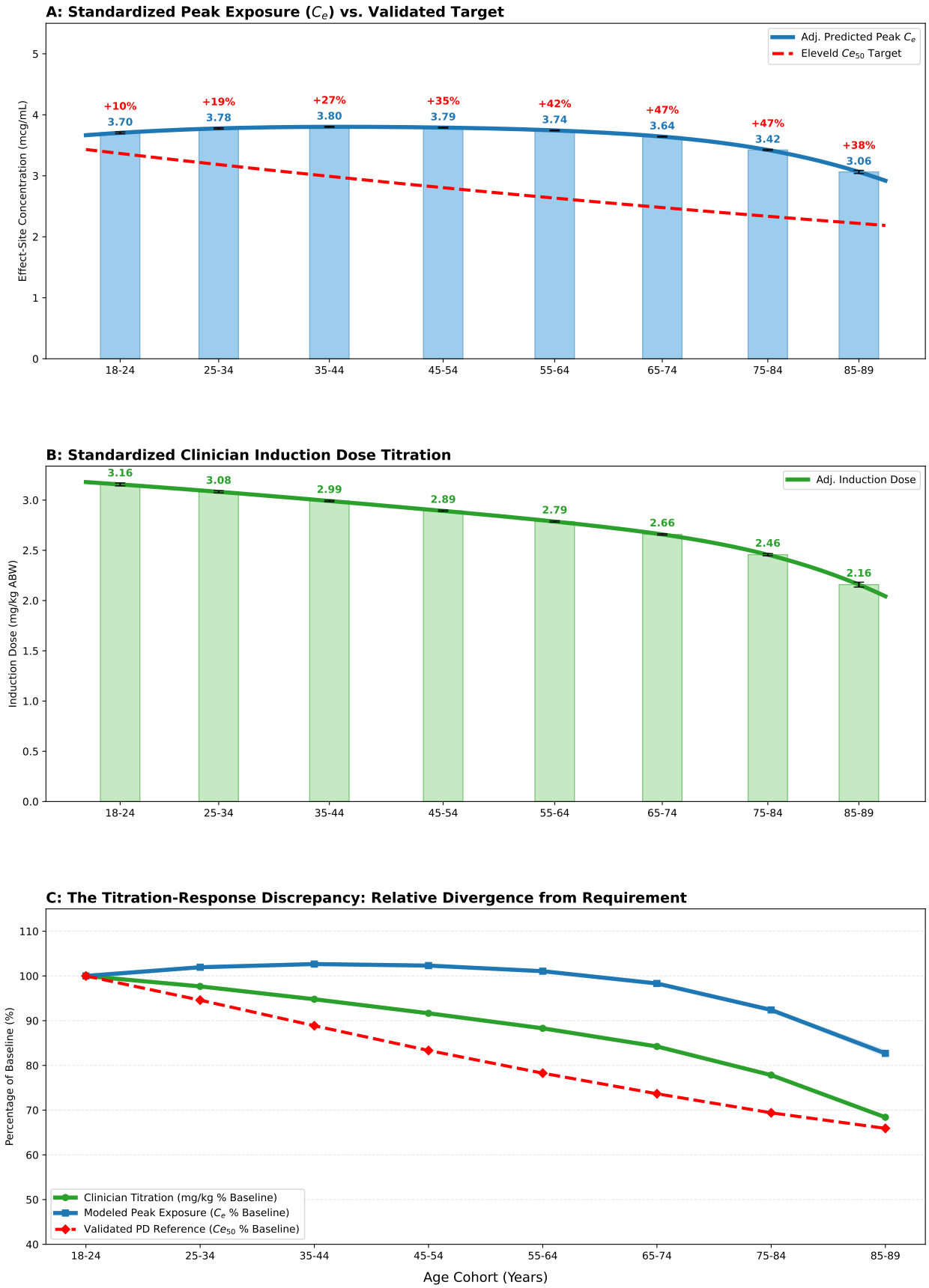

Figure 2: Multidimensional Analysis of Propofol Induction Dynamics (Continued on next page)

Figure 2: **Divergence of Clinical Dosing from Cerebral Exposure and Physiological Sensitivity. (A) Exposure vs. Requirement:** Predicted peak effect-site concentrations ($C_{e,max}$) compared to age-adjusted Ce_{50} requirements. **(B) Clinical Dosing Trajectory:** Observed weight-normalized induction doses (mg/kg) across the adult lifespan. **(C) Normalized Relative Divergence:** Relative change in clinical dosing (green), modeled exposure (blue), and biological sensitivity (red) benchmarked to the young-adult baseline (ages 18–24). **Note:** Data represent adjusted predicted means from a logistic spline model; covariates (BMI, ASA, sex) are held at population means. Shaded regions and error bars denote 95% CIs. The dashed red line indicates the Ce_{50} requirement for unconsciousness *per* Eleveld et al. Percentage labels indicate the mean exposure surplus relative to the pharmacodynamic target.

Probability of over-exposure and benchmark comparison

The probability that an individual's modeled peak effect-site exposure ($C_{e,\max}$) exceeded their age-specific Ce_{50} requirement was subsequently quantified. After adjusting for sex, BMI, and ASA physical status, logistic regression demonstrated a profound age-associated increase in the risk of over-exposure (Figure 3). For a standardized patient at age 75, the adjusted probability of $C_{e,\max}$ exceeding the age-specific Ce_{50} target was 89.6% (95% CI: 89.3–89.8%). Covariate-adjusted probabilities in the geriatric cohorts were consistently higher than raw observed proportions, indicating that age-related exposure trends persist independently of physical status or body composition.

To further contextualize these findings, the probability that an older patient's $C_{e,\max}$ exceeded the youthful Ce_{50} benchmark (3.37 $\mu g/mL$) was evaluated. While the probability of exceeding this young-adult threshold decreased with age—reflecting clinical dose reductions—the absolute frequency remained high. At age 75, the adjusted probability of achieving a peak effect-site concentration exceeding the requirement of a healthy 20-year-old was 54.7% (95% CI: 54.2–55.2%). Although weight-normalized doses were scaled down with advancing age, the resulting cerebral concentrations frequently remained at levels associated with the requirements of much younger cohorts, suggesting a persistent anchoring of geriatric titration to young-adult exposure profiles.

Validation and sensitivity analyses

Clinical face validity and TIVA Trainer comparison. To ensure the fidelity of the automated PK reconstruction, a direct comparison between the simulation pipeline and TivaTrainer was performed[22]. Representative induction sequences including a single bolus and combined bolus-infusion starts—were modeled. The reconstructed C_e trajectories demonstrated near-perfect agreement with TivaTrainer benchmarks. (Figure 4) provides a granular breakdown of these dosing schedules, confirming that this large-scale processing of the perioperative data warehouse accurately captures the non-linear C_e dynamics observed in individual clinical cases.

Robustness of the Age-Dependent Divergence. The observed divergence between achieved $C_{e,\max}$ and physiological requirements remained robust across multiple alternative model specifications and inclusion criteria:

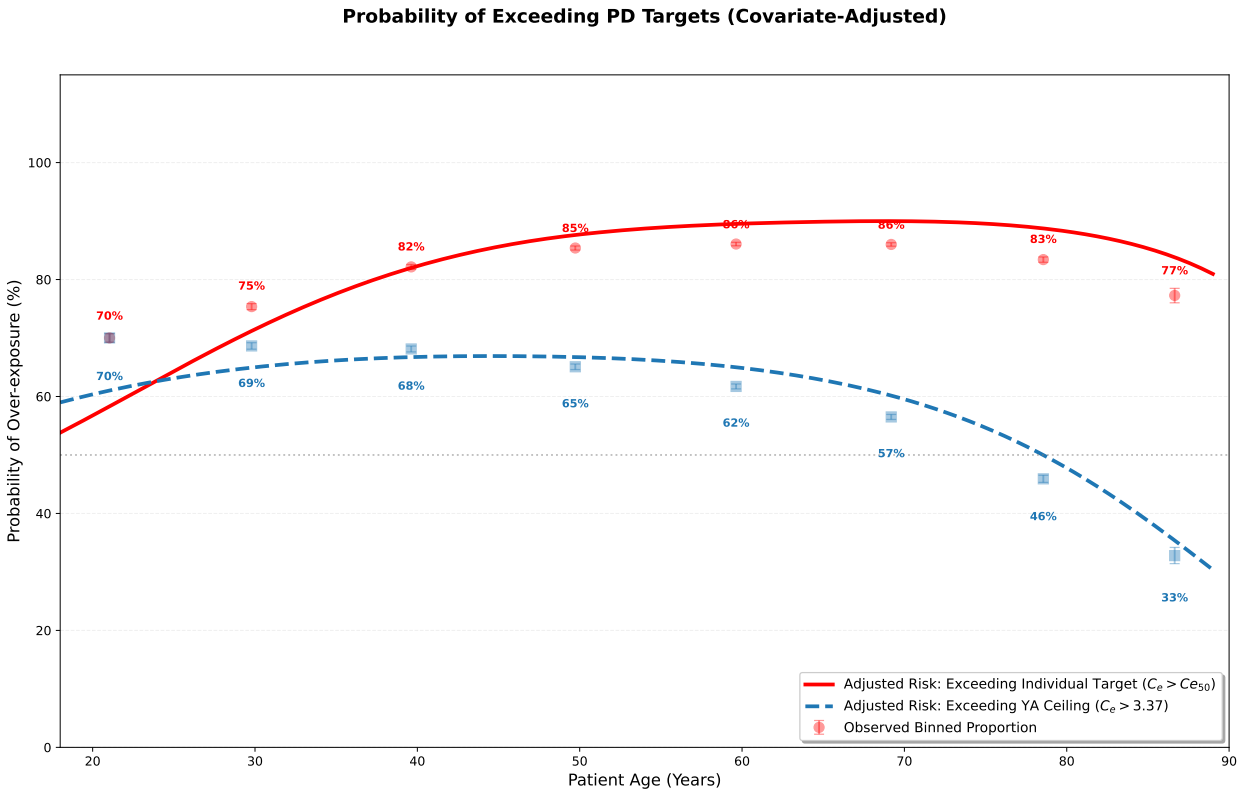

Figure 3: **Covariate-Adjusted Probability of Exceeding Pharmacodynamic Requirement Thresholds.** The red solid line illustrates the adjusted predicted probability of exceeding the individualized, age-specific physiological requirement ($C_{e,\max} > Ce_{50}$). This curve demonstrates the escalating risk of over-titration relative to biological sensitivity across the lifespan. The blue dashed line denotes the probability of exceeding a "Young Adult (YA) Ceiling"—a phenotypic benchmark defined as the Ce_{50} for the 18–24 year-old cohort—indicating the frequency with which geriatric exposures surpass even youthful standards of sensitivity. **Note:** Curves derived from logistic spline models with ASA, BMI, and sex held at population means. Binned points and error bars represent observed proportions with 95% Wilson score confidence intervals. Percentage labels indicate the raw binned observed probability at each age stratum.

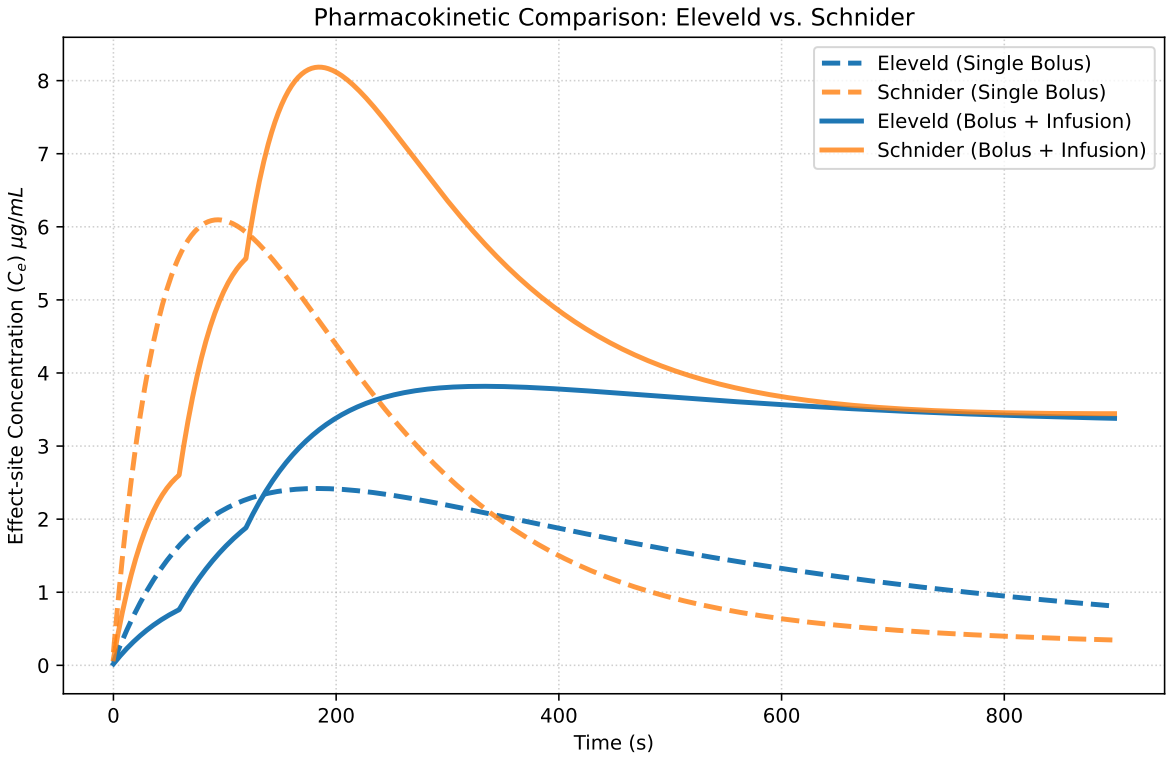

(a) Pharmacokinetic trajectories comparing the Eleveld (solid line) and Schnider (dashed line) models.

Scenario	**Age**	**S**	**Wt(kg)**	**Ht(in)**	**Timeline**	**Elev C_e**	**Schn C_e**	**TIVA-E**	**TIVA-S**
Single Bolus	65	F	65.8	65	100mg@0s	2.4	6.1	2.4	6.1
Bolus + Infusion	41	F	70.2	66	50mg@0s;50mg@60s;I:150mcg@60s;50mg@120s	3.8	8.2	3.8	8.2

(b) Comparative peak C_e values vs. TIVA Trainer benchmarks.

Figure 4: **Simulation Engine Fidelity and Model Validation.** (A) Trajectory analysis for standardized bolus and infusion regimens. (B) Benchmarking against TIVA Trainer. **Elev** C_e and **Schn** C_e represent peak concentrations calculated by the study's simulation engine; **TIVA-E** and **TIVA-S** represent independent benchmarks derived from TIVA Trainer using the Eleveld and Schnider models, respectively. The mathematical concordance between study-derived peaks and external benchmarks validates the fidelity of the retrospective simulation framework.

- **PK Model Specification:** Because PK model selection can significantly influence effect-site estimates, the primary analysis was repeated using the Schnider model[16]. While the mathematical derivations differ, the results were qualitatively identical: $C_{e,\max}$ remained persistently elevated relative to requirements, and the magnitude of the exposure-requirement mismatch increased monotonically with age (Figure S1).

- **Unadjusted Analysis:** Re-estimation of the primary models without covariate adjustment for BMI, sex, or ASA physical status yielded the same pattern of clinical over-exposure observed in the fully adjusted analysis (Figure S2).

- **Age-Grouping Sensitivity:** Incorporating the ≥ 90 year-old administrative aggregate—in which specific chronological ages were masked for de-identification—did not alter the primary findings or the slope of the exposure-requirement mismatch (Figure S3).

- **Dose Inclusion Thresholds:** Results remained unchanged when repeating the analysis with all documented propofol administrations, including cases initially flagged as outliers or those with missing dose values imputed as 0 mg (Figure S4).

The complete age-stratified summary of all sensitivity analyses, including effect-size estimates and 95% confidence intervals for each alternative model specification, is provided in Table S1. Across all configurations, the narrow confidence intervals and consistent directionality of the results confirm that the observed age-dependent exposure mismatch is a highly stable and reproducible clinical phenomenon.

DISCUSSION

In this large-scale pharmacokinetic reconstruction of over 250,000 anesthetic inductions, a profound and systematic titration-response discrepancy in geriatric propofol delivery was identified. These findings reveal that while clinicians actively reduce induction doses for older patients, these adjustments are fundamentally insufficient to prevent excessive brain exposure. This phenomenon is driven by two primary factors: first, the maintenance of an absolute dosing baseline that mirrors standard young-adult practice—frequently doubling the 1.0–1.5 mg/kg recommended in geriatric guidelines—and second, a pharmacokinetic "decoupling" in which weight-based dose reductions fail to translate into commensurate reductions in peak effect-site concentration ($C_{e,\max}$).

The most salient feature of these results is the resistance of the achieved $C_{e,\max}$ to clinical titration, a phenomenon driven by a profound pharmacokinetic "decoupling." While the 32% reduction in clinician dosing nominally mirrors the 34% decline in biological requirement, the resulting reduction in peak cerebral exposure (17%) lags significantly behind both (Figure 2C). This mismatch is consistent with known age-associated physiological shifts—specifically the contraction of the central distribution volume, altered intercompartment kinetics, and diminished metabolic clearance—which effectively "undo" nearly half of the clinician's intended dose reduction. Consequently, the adjusted $C_{e,\max}$ curve

demonstrates only a limited decline through much of adulthood, while the physiological requirement (Ce_{50}) drops steadily and exponentially (Figure 2A). Collectively, this widening offset provides a robust signal of a systematic titration failure that transcends the absolute accuracy of any single model; regardless of model selection, mg/kg scaling remains a fundamentally imprecise tool for tracking the steepening curve of geriatric sensitivity.

A key implication of this work is that weight-normalized dosing—even when ostensibly adjusted for age—serves as an incomplete surrogate for physiologic exposure. Conventional mg/kg metrics fail to capture how age-dependent distribution and clearance kinetics dictate the actual peak brain exposure. By reconstructing C_e from real-world delivery sequences, this study provides a mechanistic estimate of modeled effect-site concentration which more closely approximates the clinical quantity anesthesiologists are ultimately attempting to control. These findings illustrate that the gap between practice and physiology is larger than mg/kg metrics alone would imply; while dose-based data suggests over-administration relative to guidelines, the exposure-based framework reveals a significantly more profound and persistent clinical overshoot.

Robustness across model and analytic choices

The identified titration-response discrepancy remains robust across a wide range of modeling assumptions and sensitivity analyses, suggesting it is a fundamental property of clinical practice rather than an artifact of any single pharmacokinetic specification. A sensitivity analysis utilizing the Schnider model demonstrated qualitatively identical age-associated exposure mismatches, despite its differing mathematical approach to age-related volumes and clearances. Furthermore, the pattern of persistently elevated $C_{e,\max}$ remained consistent in unadjusted analyses, in evaluations of the masked $\geq$ 90-year-old cohort, and in unfiltered models that included data outliers and missing propofol administrations. These results confirm that the age-dependent exposure mismatch is a stable signal that persists regardless of covariate handling, data imputation, or inclusion criteria, providing high confidence in the internal validity of the simulation pipeline.

Comparison to prior literature and novelty

While previous literature has noted that clinicians frequently exceed weight-based geriatric recommendations[4], this work extends the understanding of induction safety in three significant ways.First, by evaluating induction practice through the lens of modeled effect-site exposure (C_e) rather than simple mg/kg metrics, a latent elevation in cerebral exposure is identified. It is demonstrated that even when weight-based dose reductions are performed, pharmacokinetic shifts in the elderly effectively negate a significant portion of that effort, resulting in cerebral drug levels that remain anchored to young-adult targets.Second, the dynamic complexity of real-world induction is captured through this reconstruction. In contrast to previous studies that often assume a single, static bolus, cumulative exposure is reconstructed here from fragmented boluses and infusion starts. This reveals that the observed overshoot is not limited to the "initial push," but is a characteristic of the entire induction sequence.Third, a high-resolution lifespan mapping of the titration-response discrepancy is provided. Rather than comparing broad age categories (e.g., "young" vs. "old"), the precise

age-associated divergence is characterized across the adult spectrum. This allows for the identification of the specific decades where clinician titration fails to track physiological requirements, demonstrating that the titration offset is a progressive phenomenon that begins earlier and persists more consistently than previously recognized.

Clinical implications

The identified age-dependent titration offset has direct relevance to perioperative safety, particularly regarding hemodynamic stability and neurocognitive outcomes in an increasingly elderly surgical population. Excessive cerebral propofol concentrations during the dynamic induction phase are primary drivers of post-induction hypotension[8,23], a known risk factor for myocardial and acute kidney injury. Furthermore, elevated effect-site concentrations are strongly associated with the occurrence of EEG burst suppression. While it is debated whether burst suppression is a direct mediator of postoperative neurocognitive disorders or an epiphenomenon of cerebral frailty, its presence is a validated indicator of inadequately high anesthetic administration.[24–26]A transition toward neurophysiologically-informed anesthetic administration is supported by the magnitude of the identified titration offset. Rather than serving as a prescriptive, age-based target for individual titration, the Ce_{50} benchmarks utilized in this analysis are positioned as a critical "wake-up call"—a signal that current weight-based practices result in drug delivery that is fundamentally misaligned with geriatric physiology. These findings suggest that weight-normalized (mg/kg) dosing remains an unreliable surrogate for cerebral exposure in older adults, especially during the rapid transitions of induction. The integration of real-time EEG monitoring provides a specific window into the hypnotic state, facilitating a more thoughtful administration that is calibrated to the patient's actual neurophysiologic sensitivity rather than an imprecise weight-based estimate. Such a shift may be necessary to minimize the excessive induction intensity that currently characterizes geriatric anesthesia and to better protect this vulnerable cohort from avoidable cortical depression.

Limitations

Several limitations of this study warrant consideration. First, as a retrospective model-based analysis, reliance is placed on the accuracy of electronic health record (EHR) timestamps and the generalizability of the Eleveld parameterization. While documentation errors could affect individual C_e estimates, the scale and consistency of the observed signal suggest that such errors are unlikely to account for the broad population-level trends.Second, the Ce_{50} reference represents a population-averaged hypnotic requirement rather than a personalized target. This study utilized the propofol-only parameterization of the Eleveld model to provide a standardized physiological benchmark across the age spectrum. Second, while some literature suggests potential model bias in the elderly[27], the magnitude of the observed titration offset is significantly larger than any reported model-specific bias. Furthermore, the qualitative replication of these findings using the Schnider architecture—which utilizes a different mathematical approach to age-related volumes and clearances—suggests that the identified discrepancy is a robust clinical signal that transcends any single parameterization. Because both the achieved $C_{e,\max}$ and the Ce_{50} reference share the same mathematical foundations, any potential systematic bias in the geriatric estimates is inherently controlled for

in the relative comparison.Finally, the single-center nature of this investigation may limit its external validity, as anesthetic titration habits and institutional protocols for geriatric patients may vary significantly between healthcare systems.

Translational Value of Exposure-Based Modeling

The methodology employed here offers a framework for evaluating the discrepancy between administered dose and physiologic exposure across the perioperative period. Traditional database research frequently relies on total drug mass as a proxy for clinical effect; however, these findings demonstrate that weight-normalized dosing is a limited surrogate that fails to capture significant age-related elevations in cerebral exposure. This exposure-informed framework is readily applicable to other perioperative agents—such as opioids or dexmedetomidine—where the temporal concentration at the effect-site is often more clinically relevant than the cumulative quantity administered.

Conclusions

In this high-resolution analysis of over 250,000 cases, a systematic failure to down-titrate propofol exposure in the aging brain was demonstrated. While clinicians actively reduce mg/kg doses with age, these adjustments are fundamentally mismatched with the exponential increase in geriatric hypnotic sensitivity. The resulting exposure-requirement gap is not a subtle deviation but a profound, population-wide overshoot that leaves the vast majority of older adults at risk of excessive anesthesia. Ultimately, our results suggest that the current reliance on weight-normalized induction heuristics is insufficient. Moving toward a model-informed understanding of effect-site exposure may be the necessary step to bridge the gap between clinical intent and physiological safety in the geriatric population.

DATA AVAILIBILITY

The source code for the pharmacokinetic reconstruction and statistical analysis is hosted on GitHub and will be made publicly available upon peer-reviewed publication. During the preprint phase, code is available from the corresponding author upon reasonable request.

DECLARATION OF GENERATIVE AI AND AI-ASSISTED TECHNOLOGIES IN THE WRITING PROCESS

During the preparation of this work, the author utilized Large Language Models (Gemini 3.1 Pro and GPT-5.2 Thinking) in order to assist in the translation of research-derived pseudocode into Python-based analytic scripts. The primary investigator provided the underlying physiological logic, defined all pharmacokinetic modeling parameters, and directed the iterative development process through sequential technical prompting. After using these tools, the author reviewed and edited the generated code as needed; specifically, all AI-assisted scripts were manually audited for syntax and logical errors, debugged for domain-specific accuracy, and validated against known benchmark calculations to ensure the integrity of the data processing pipeline. The author takes full responsibility for the content of the publication.

References

1. Prince, M. J., Wu, F., Guo, Y., Gutierrez Robledo, L. M., O'Donnell, M., Sullivan, R. & Yusuf, S. The burden of disease in older people and implications for health policy and practice. *The Lancet* **385,** 549–562 (Feb. 2015).
2. Deiner, S., Westlake, B. & Dutton, R. P. Patterns of Surgical Care and Complications in Elderly Adults. *Journal of the American Geriatrics Society* **62,** 829–835 (May 2014).
3. Becher, R. D., Vander Wyk, B., Leo-Summers, L., Desai, M. M. & Gill, T. M. The Incidence and Cumulative Risk of Major Surgery in Older Persons in the United States. *Annals of Surgery* **277,** 87–92 (Jan. 2023).
4. Yang, H., Deng, H.-M., Chen, H.-Y., Tang, S.-H., Deng, F., Lu, Y.-G. & Song, J.-C. The Impact of Age on Propofol Requirement for Inducing Loss of Consciousness in Elderly Surgical Patients. *Frontiers in Pharmacology* **13,** 739552 (Mar. 28, 2022).
5. Schnider, T. W., Minto, C. F., Shafer, S. L., Gambus, P. L., Andresen, C., Goodale, D. B. & Youngs, E. J. The Influence of Age on Propofol Pharmacodynamics. *Anesthesiology* **90,** 1502–1516. (June 1, 1999).
6. *Propofol Injection, Emulsion [package insert]. U.S. Food and Drug Administration* https://fda.report/DailyMed/fdb77e13-f5a7-4c4a-9f8e-338b702239c8/. Accessed February 20, 2026 (U.S. Food and Drug Administration).
7. Schonberger, R. B., Bardia, A., Dai, F., Michel, G., Yanez, D., Curtis, J. P., Vaughn, M. T., Burg, M. M., Mathis, M., Kheterpal, S., Akhtar, S. & Shah, N. Variation in Propofol Induction Doses Administered to Surgical Patients over Age 65. *Journal of the American Geriatrics Society* **69,** 2195–2209 (Aug. 2021).
8. Phillips, A. T., Deiner, S., Lin, H. M., Andreopoulos, E., Silverstein, J. & Levin, M. A. Propofol Use in the Elderly Population: Prevalence of Overdose and Association With 30-Day Mortality. *Clinical therapeutics* **37,** 2676–2685 (Dec. 1, 2015).
9. Akhtar, S., Liu, J., Heng, J., Dai, F., Schonberger, R. B. & Burg, M. M. Does intravenous induction dosing among patients undergoing gastrointestinal surgical procedures follow current recommendations: a study of contemporary practice. *Journal of Clinical Anesthesia* **33,** 208–215 (Sept. 2016).
10. Chen, E. Y., Michel, G., Zhou, B., Dai, F., Akhtar, S. & Schonberger, R. B. An Analysis of Anesthesia Induction Dosing in Female Older Adults. *Drugs & Aging* **37,** 435–446 (June 2020).
11. Al-Rifai, Z. & Mulvey, D. Principles of total intravenous anaesthesia: practical aspects of using total intravenous anaesthesia. *BJA Education* **16,** 276–280 (Aug. 2016).
12. Vandemoortele, O., Hannivoort, L. N., Vanhoorebeeck, F., Struys, M. M. R. F. & Vereecke, H. E. M. General Purpose Pharmacokinetic-Pharmacodynamic Models for Target-Controlled Infusion of Anaesthetic Drugs: A Narrative Review. *Journal of Clinical Medicine* **11,** 2487 (Apr. 28, 2022).

13. Eleveld, D., Colin, P., Absalom, A. & Struys, M. Pharmacokinetic–pharmacodynamic model for propofol for broad application in anaesthesia and sedation. *British Journal of Anaesthesia* **120,** 942–959 (May 2018).

14. Hofer, I. S., Gabel, E., Pfeffer, M., Mahbouba, M. & Mahajan, A. A Systematic Approach to Creation of a Perioperative Data Warehouse. *Anesthesia & Analgesia* **122,** 1880–1884 (June 2016).

15. Mathiszig-Lee, J. *PyTCI: Open-source Target-Controlled Infusion simulation library.* https://github.com/JMathiszig-Lee/PyTCI. 2022.

16. Schnider, T. W., Minto, C. F., Gambus, P. L., Andresen, C., Goodale, D. B., Shafer, S. L. & Youngs, E. J. The Influence of Method of Administration and Covariates on the Pharmacokinetics of Propofol in Adult Volunteers. *Anesthesiology* **88,** 1170–1182 (May 1, 1998).

17. Van Rossum, G. & Drake, F. *Python Programming Language* version 3.12.12. 2009.

18. McKinney, W. *Data Structures for Statistical Computing in Python* in. Python in Science Conference (Austin, Texas, 2010), 56–61.

19. Harris, C. R., Millman, K. J., Van Der Walt, S. J., Gommers, R., Virtanen, P., Cournapeau, D., Wieser, E., Taylor, J., Berg, S., Smith, N. J., Kern, R., Picus, M., Hoyer, S., Van Kerkwijk, M. H., Brett, M., Haldane, A., Del Río, J. F., Wiebe, M., Peterson, P., Gérard-Marchant, P., Sheppard, K., Reddy, T., Weckesser, W., Abbasi, H., Gohlke, C. & Oliphant, T. E. Array programming with NumPy. *Nature* **585,** 357–362 (Sept. 17, 2020).

20. Seabold, S. & Perktold, J. *Statsmodels: Econometric and Statistical Modeling with Python* in. Python in Science Conference (Austin, Texas, 2010), 92–96.

21. Smith, N. J., Broessli, Skipper Seabold & Davidson-Pilon, C. *patsy v0.2.1* version v0.2.1. Aug. 26, 2014.

22. Engbers, F. *TIVAtrainer* version 3.1.1. 2026.

23. Dundee, J. W., Robinson, F. P., McCOLLUM, J. S. C. & Patterson, C. C. Sensitivity to propofol in the elderly. *Anaesthesia* **41,** 482–485 (May 1986).

24. Obert, D. P., Sepúlveda, P. O., Adriazola, V., Zurita, F., Brouse, J., Schneider, G. & Kreuzer, M. Overcoming age: Slow anesthesia induction may prevent geriatric patients from developing burst suppression and help developing intraoperative EEG signatures of a younger brain. *Journal of Clinical Anesthesia* **99,** 111672 (Dec. 1, 2024).

25. Purdon, P., Pavone, K., Akeju, O., Smith, A., Sampson, A., Lee, J., Zhou, D., Solt, K. & Brown, E. The Ageing Brain: Age-dependent changes in the electroencephalogram during propofol and sevoflurane general anaesthesia. *British Journal of Anaesthesia* **115,** i46–i57 (July 2015).

26. Fritz, B. A., King, C. R., Ben Abdallah, A., Lin, N., Mickle, A. M., Budelier, T. P., Oberhaus, J., Park, D., Maybrier, H. R., Wildes, T. S., Avidan, M. S. & for the ENGAGES Research Group*. Preoperative Cognitive Abnormality, Intraoperative Electroencephalogram Suppression, and Postoperative Delirium: A Mediation Analysis. *Anesthesiology* **132,** 1458–1468 (June 2020).

27. Vellinga, R., Hannivoort, L. N., Introna, M., Touw, D. J., Absalom, A. R., Eleveld, D. J. & Struys, M. M. F. Prospective clinical validation of the Eleveld propofol pharmacokinetic-pharmacodynamic model in general anaesthesia. *British Journal of Anaesthesia* **126,** 386–394 (Feb. 2021).

SUPPLEMENTAL TABLES AND FIGURES

Table S1: **Robustness of Age-Associated Titration Offsets across Alternative Modeling and Inclusion Criteria.**

Age Cohort	N	Dose (mg/kg)	Peak C_e	Surplus %
Arithmetic (Raw) Analysis				
18-24	14,983	3.26 (3.24–3.28)	3.97 (3.95–3.99)	17.9% (17.3–18.5%)
25-34	27,186	3.16 (3.15–3.17)	3.91 (3.89–3.92)	22.8% (22.3–23.2%)
35-44	33,599	3.07 (3.06–3.08)	3.87 (3.86–3.89)	29.5% (29.1–29.9%)
45-54	39,747	2.92 (2.91–2.93)	3.77 (3.76–3.79)	34.6% (34.2–34.9%)
55-64	51,731	2.75 (2.74–2.76)	3.68 (3.67–3.69)	39.8% (39.4–40.1%)
65-74	52,869	2.60 (2.59–2.61)	3.57 (3.56–3.58)	43.8% (43.5–44.2%)
75-84	25,962	2.36 (2.35–2.37)	3.32 (3.31–3.34)	42.3% (41.7–42.9%)
85+*	4,440	2.08 (2.05–2.10)	2.99 (2.96–3.02)	34.6% (33.2–36.0%)
Inclusion of Outliers				
18-24	15,107	3.15 (3.13–3.16)	3.70 (3.68–3.71)	9.8% (9.4–10.3%)
25-34	27,399	3.08 (3.07–3.09)	3.77 (3.76–3.78)	18.4% (18.0–18.8%)
35-44	33,879	2.99 (2.98–2.99)	3.80 (3.79–3.80)	26.9% (26.6–27.2%)
45-54	40,113	2.89 (2.88–2.89)	3.78 (3.77–3.79)	34.9% (34.6–35.2%)
55-64	52,182	2.78 (2.77–2.79)	3.74 (3.73–3.74)	41.8% (41.5–42.1%)
65-74	53,334	2.65 (2.64–2.66)	3.63 (3.63–3.64)	46.6% (46.3–46.9%)
75-84	26,174	2.45 (2.44–2.46)	3.41 (3.40–3.43)	46.2% (45.7–46.7%)
85+*	4,497	2.15 (2.13–2.18)	3.05 (3.02–3.08)	37.5% (36.3–38.7%)
Age 90+ Extended Analysis				
18-24	14,920	3.15 (3.14–3.17)	3.70 (3.69–3.72)	10.1% (9.6–10.5%)
25-34	27,066	3.08 (3.07–3.09)	3.78 (3.76–3.79)	18.6% (18.2–19.0%)
35-44	33,458	2.99 (2.98–3.00)	3.80 (3.79–3.81)	27.1% (26.9–27.4%)
45-54	39,560	2.89 (2.88–2.90)	3.79 (3.78–3.80)	35.1% (34.8–35.4%)
55-64	51,488	2.79 (2.78–2.79)	3.74 (3.74–3.75)	42.1% (41.8–42.4%)
65-74	52,577	2.66 (2.65–2.66)	3.64 (3.64–3.65)	46.9% (46.6–47.2%)
75-84	25,809	2.46 (2.45–2.47)	3.42 (3.41–3.44)	46.6% (46.1–47.1%)
85+*	6,446	2.10 (2.08–2.12)	2.98 (2.96–3.00)	35.2% (34.1–36.2%)
Schnider PK Model				
18-24	14,941	3.16 (3.14-3.17)	9.24 (9.20-9.28)	—
25-34	27,088	3.08 (3.07-3.09)	9.55 (9.53-9.58)	—
35-44	33,469	2.99 (2.98-3.00)	9.73 (9.71-9.75)	—
45-54	39,583	2.89 (2.88-2.90)	9.80 (9.78-9.82)	—
55-64	51,510	2.79 (2.78-2.79)	9.78 (9.76-9.80)	—
65-74	52,594	2.66 (2.65-2.67)	9.57 (9.56-9.59)	—
75-84	25,816	2.46 (2.45-2.47)	9.08 (9.05-9.11)	—
85+*	4,419	2.16 (2.13-2.18)	8.31 (8.24-8.37)	—

Note: Values represent covariate-adjusted means (95% CI). $C_{e,\max}$: peak effect-site concentration (μg/mL). The "Relative Offset" indicates the percentage by which modeled exposure exceeds the age-adjusted Eleveld Ce_{50} benchmark. Sensitivity scenarios include: (1) alternative pharmacokinetic parameterization using the Schnider model; (2) unadjusted (raw) population analysis; and (3) an unfiltered cohort incorporating physiological outliers, missing propofol records (imputed as 0 mg), and the inclusion of the "masked" geriatric population (ages $\geq$90).

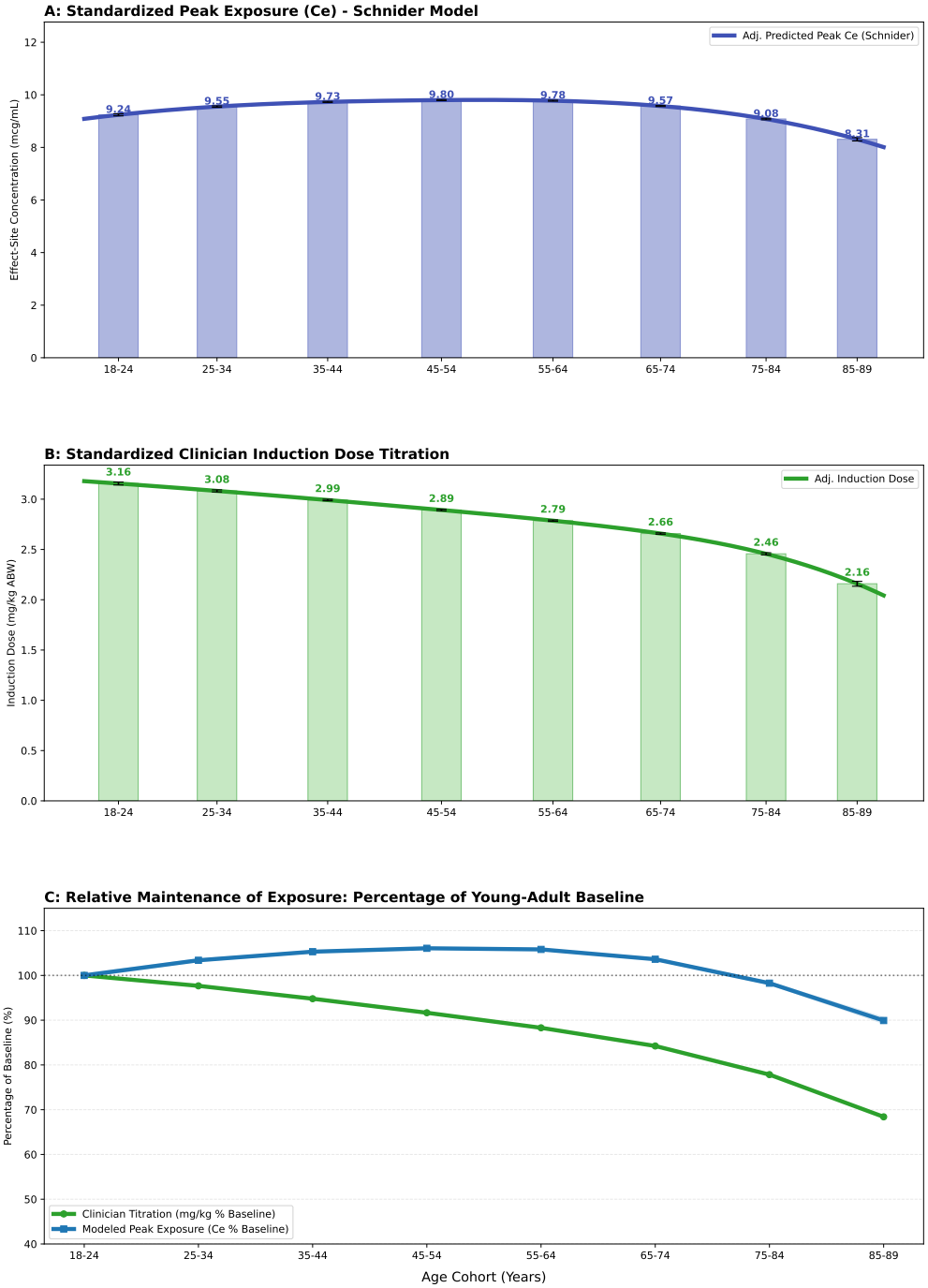

Figure S1: **Model Sensitivity Analysis Using Schnider Parameters**

Secondary analysis confirming that observed exposure trends are independent of the primary pharmacokinetic parameterization. **(A) Peak Effect-Site Exposure (C_e):** Predicted concentrations using the Schnider model; exposure remains elevated in geriatric patients despite significantly increased pharmacodynamic sensitivity. **(B) Relative Divergence:** Normalization to the 18–24 year-old baseline illustrates the titration offset: while clinician dosing (green) decreases, the resulting cerebral exposure (blue) remains relatively fixed across the lifespan. Error bars denote 95% CI.

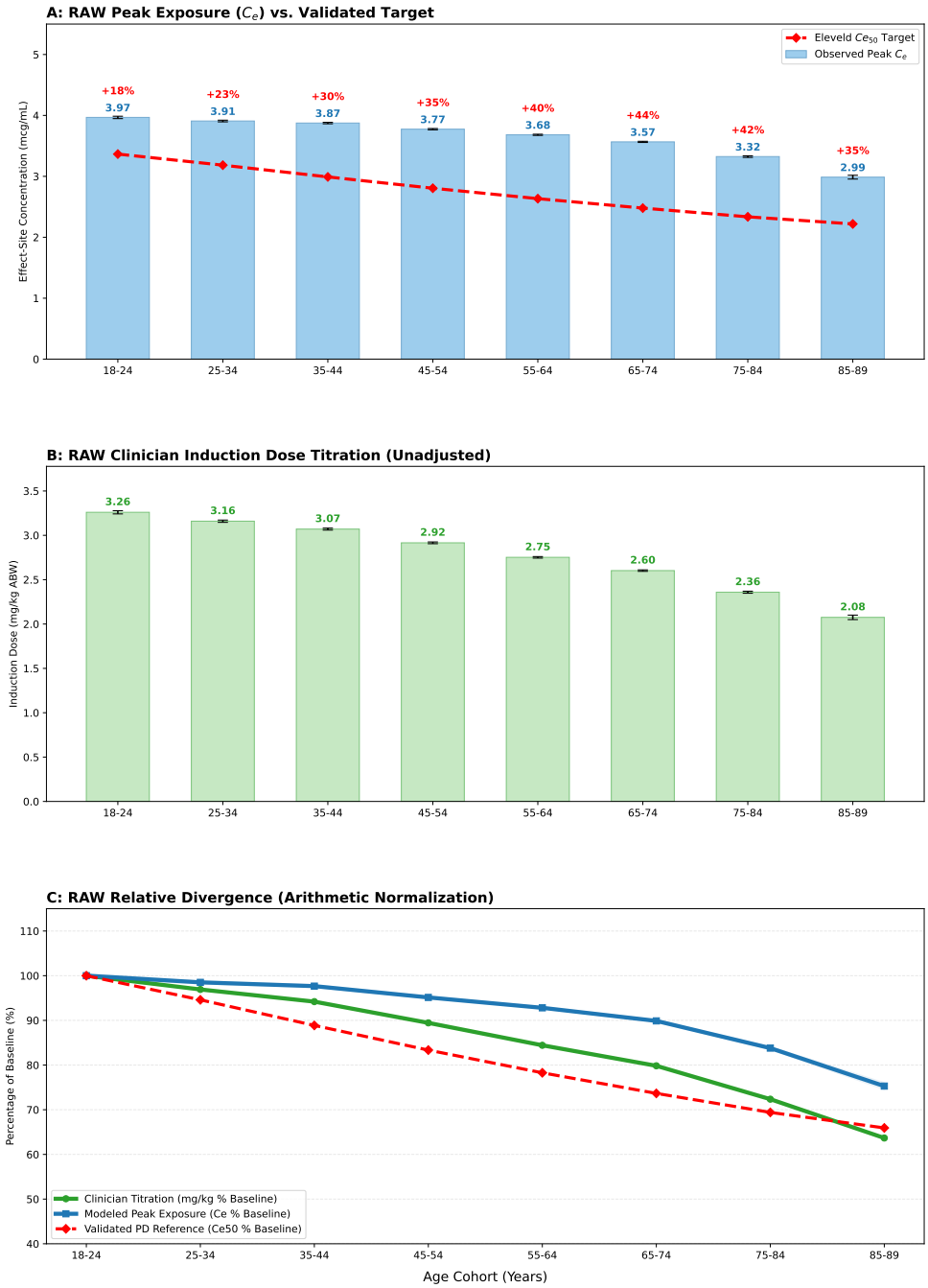

Figure S2: **Population-Level Analysis of Unadjusted (Raw) Clinical Propofol Dynamics**

Arithmetic means derived from EHR documentation illustrate the divergence between practice and physiological requirements prior to covariate standardization. **(A) Peak Brain Exposure (C_e) vs. Target:** Observed C_e (blue) compared to age-adjusted Eleveld Ce_{50} (red) **(B) Clinician Induction Dose Titration:** Administered doses (mg/kg) follow a linear reduction trend that fails to compensate for exponential increases in brain sensitivity. **(C) Relative Divergence:** Normalized variables indexed to the 18–24 year-old baseline. Error bars denote 95% CI.

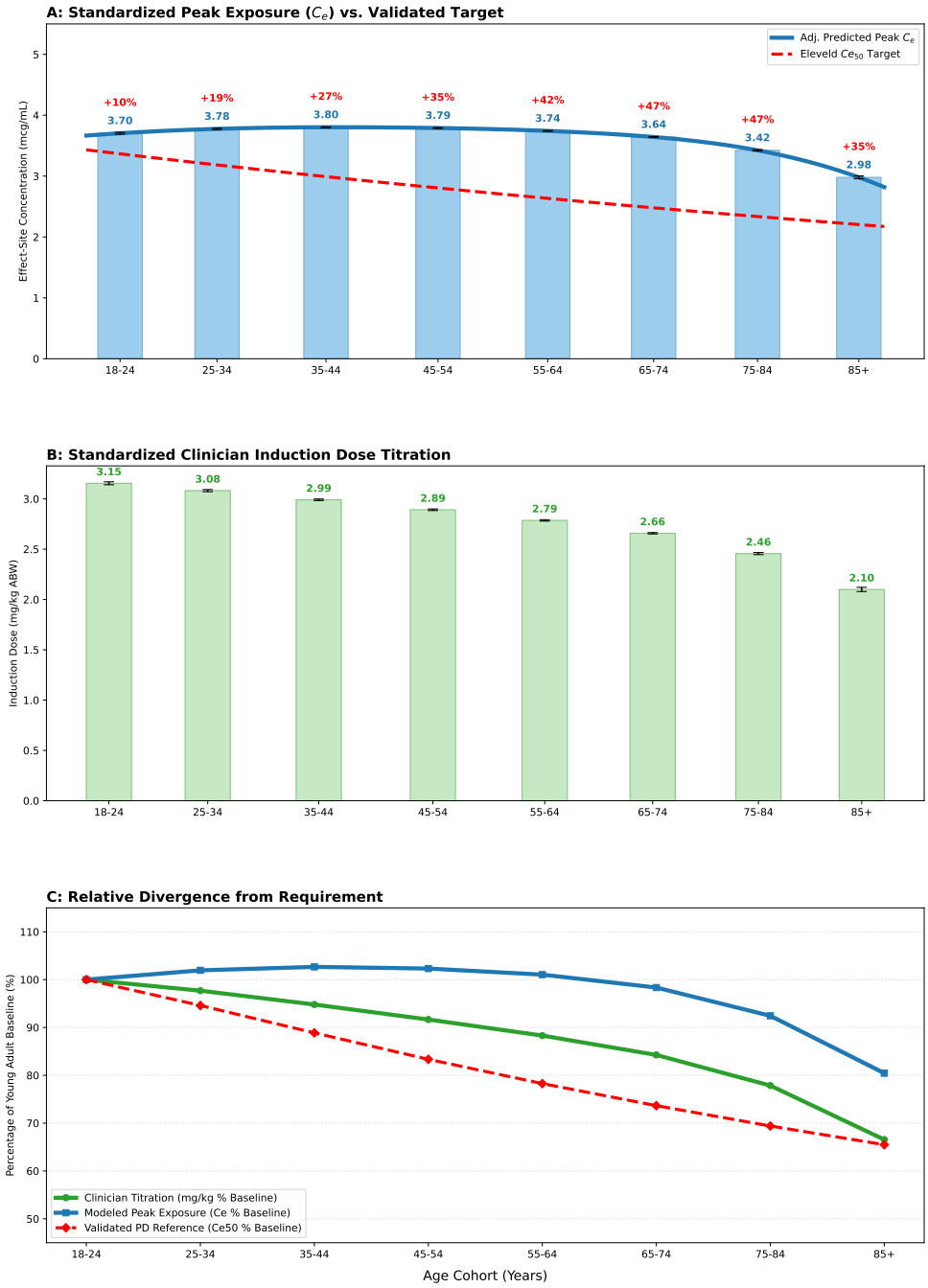

Figure S3: **Sensitivity Analysis Including Patients Aged 90 and Older**

Standardized population-level dynamics including the advanced geriatric population. **(A) Standardized Peak Exposure (C_e):** Observed exposure (blue) versus Eleveld Ce_{50} requirement (red). **(B) Standardized Dose Titration:** Administered induction doses (mg/kg) across the full lifespan. **(C) Standardized Relative Divergence:** Error bars denote 95% CI.

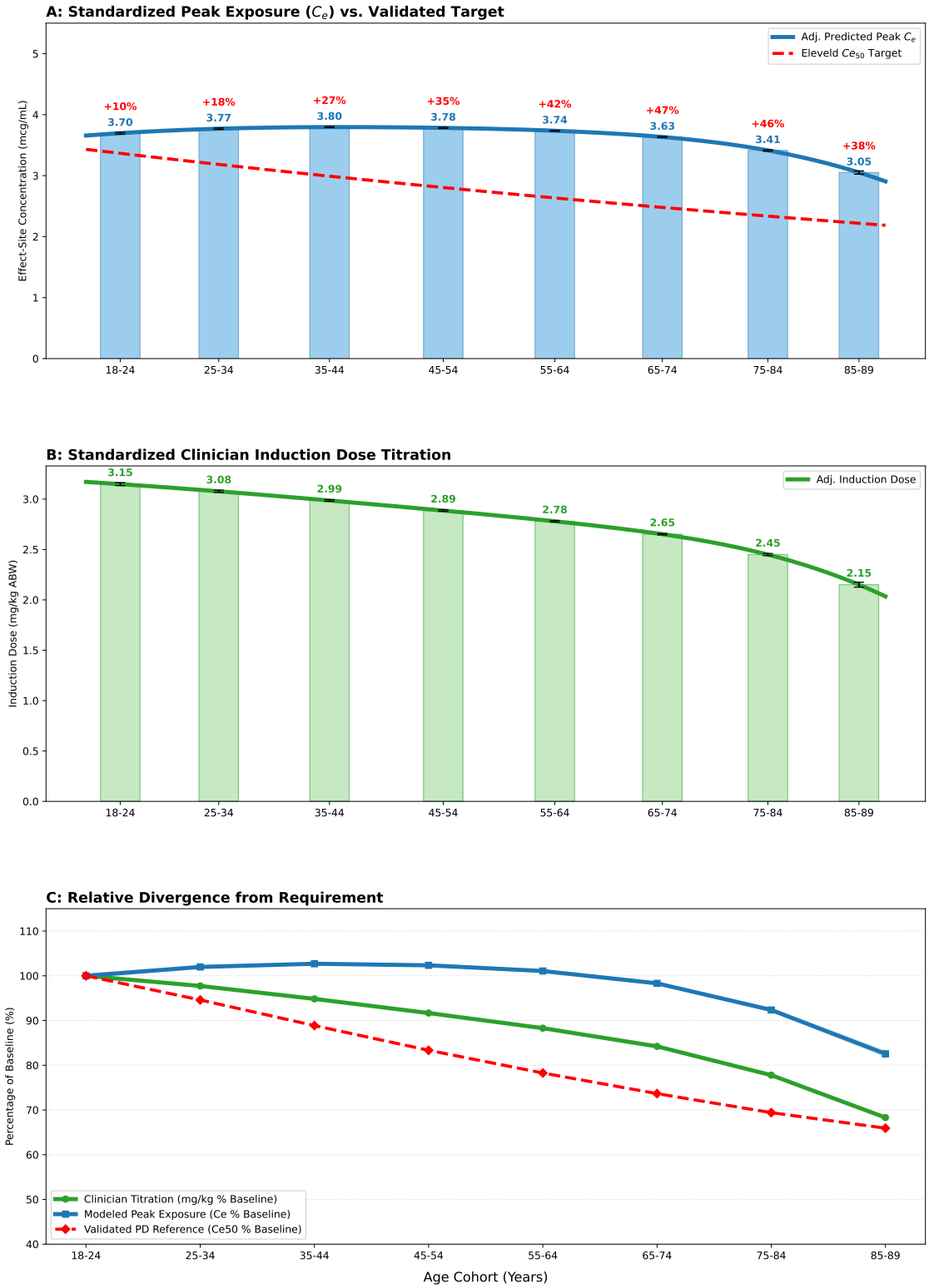

Figure S4: Sensitivity Analysis of the Titration-Response Discrepancy with Outlier Inclusion. (A) Standardized peak C_e vs. Eleveld Ce_{50} targets; (B) Clinician induction dose titration (mg/kg); (C) Relative divergence from baseline requirement. The inclusion of outliers and imputed missing data (missing doses set to zero) confirms that the progressive age-related over-exposure observed in the primary analysis remains robust across different data-filtering strategies.